Research Square

Preprints are preliminary reports that have not undergone peer review.
They should not be considered conclusive, used to inform clinical practice,
or referenced by the media as validated information.

Vibrational Intensification of Mass Transfer Across the Interface Between Viscous Liquids

O. A. VLASOVA

vlasova_oa@pspu.ru

Perm State Humanitarian Pedagogical University

A. A. VJATKIN

Perm State Humanitarian Pedagogical University

V. G. KOZLOV

Perm State Humanitarian Pedagogical University

Research Article

Keywords: viscous liquid, interface, vibrations, mean flow, mass transfer

Posted Date: November 11th, 2026

DOI: https://doi.org/10.21203/rs.3.rs-11507451/v1

License: This work is licensed under a Creative Commons Attribution 4.0 International License.
Read Full License

Additional Declarations: No competing interests reported.

VIBRATIONAL INTENSIFICATION OF MASS TRANSFER ACROSS THE INTERFACE BETWEEN VISCOUS LIQUIDS

O.A. VLASOVA, A.A. VJATKIN, V.G. KOZLOV
vlasova_oa@pspu.ru[1]
ORCID 0000-0003-2200-7441
Laboratory of Vibrational Hydromechanics,
Perm State Humanitarian Pedagogical University,
614990, Perm, Sibirskaya Str., 24

Abstract: Vibrations are an effective tool for controlling fluid motion and mass transfer, in particular under microgravity conditions. The study addresses a topical technological problem: the intensification of mass transfer across the interface between immiscible high-viscosity liquids. The time-averaged flow in a flat vertical cell, generated by oscillations of a body at the interface between two viscous fluids, is investigated experimentally. The body has the shape of a parallelepiped elongated along the interface, with straight (beveled) edges. It is found that oscillations of the body perpendicular to the interface induce intense time-averaged flows in the form of a pair of large-scale vortices in each fluid, encompassing the entire cell volume. The flow direction is opposite to that of the known case of steady streaming in low-viscosity fluids. The dependence of the structure and intensity of the time-averaged flows on the vibration parameters is determined. It is shown that the detected time-averaged flow intensifies the mass transfer of a substance dissolved in one of the fluids across the interface; the mass transfer rate exceeds the diffusion rate by several orders of magnitude. The discovered vibration-induced effect is novel and can be effectively used in technological processes, in particular under reduced gravity conditions.

Key words: viscous liquid, interface, vibrations, mean flow, mass transfer.

Introduction

The problem of mass transfer at the interface and its intensification is one of the most important issues in chemical and biological technologies (Denisova and Kostarev 2022; Volodin and Alabuzhev 2025; Denisova et al. 2026). Interest in this area is due to the large number of technological applications and problems. The widespread occurrence of multiphase systems with interfaces makes the task of controlling the interface, its shape, and the flows arising in the contacting media near the interface particularly urgent. Vibrations are an effective tool for influencing interfaces: on the one hand, they affect the interface shape; on the other, they can generate intense mean flows on either side of the interface (Lyubimov et al. 2003). It should be noted that flows near the interface play a crucial role in interfacial mass transfer, since they change the mass transfer regime from diffusive to convective.

A brief consideration is given to the mean flows generated by fluid oscillations. Flows excited by liquid (gas) oscillations are a phenomenon that has attracted the attention of many scientists, dating back to Lord Rayleigh (1884) and has been described in monographs (Landau and Lifschitz 1959; Nyborg 1965; Batchelor 1967). Mean flows arise from inhomogeneous Stokes layers; they have been termed "steady streaming" and have been extensively studied theoretically and experimentally (Schlichting 1951; Nyborg 1965; Riley 1966; Riley 2001). Thus, for translational oscillations of a body (e.g., a sphere) in an incompressible fluid, a secondary flow forms outside the thin Stokes boundary layers on the body surface, in the form of two jets directed away from the body along the oscillation axis (Van Dyke 1982). In this case, large-scale axisymmetric toroidal vortical flows are generated in the liquid. A similar situation occurs when an oscillating body is located at a free surface or at the interface between liquids (Taneda 1991; Taneda 1994; Ivanova et al. 1998; Lyubimova et al. 2025). In this case, a further mechanism is added: the generation of mean flows in the boundary layers at the interface, i.e., the Long–Higgins mechanism (Lyubimov et al. 2003).

It is important to note that most studies are devoted to low-viscosity liquids and high dimensionless oscillation frequencies, i.e., the limiting case of Stokes layers that are thin compared with the characteristic body dimensions. The ratio of the characteristic body (cavity) size h to the Stokes boundary layer thickness $\delta \equiv (2\nu/\Omega)^{0.5}$ is characterized by the dimensionless frequency $\omega \equiv \Omega h^2/\nu$. Here ν is the kinematic viscosity of the fluid, and Ω is the oscillation frequency. A number of theoretical and experimental studies have addressed flows as a function of the dimensionless frequency. The mean flows in the transition and low-frequency ranges, and in particular their effect on heat and mass transfer, have been studied in deformable phase inclusions whose boundaries undergo oscillations of various types (Kozlov et al. 2017; Sabirov et al. 2018; Subbotin et al. 2018; Kozlov 2019). In all the examples described, in the low-frequency range the structure of the mean flows is reversed compared with the high-frequency limit. Moreover, with increasing viscosity (with decreasing dimensionless oscillation frequency), the intensity of the mean flows decreases proportionally.

Let us return to the mean flows near the interphase (free boundary). Recall that wave processes at the interface can also generate mean flows (Lyubimov et al. 2003). This is observed primarily in low-viscosity liquids.

[1] Email address for corresponding author: vlasova_oa@pspu.ru

The viscous interaction of liquids during oscillations of the interface with the solid cavity walls, as occurs in narrow slit channels (Hele-Shaw cells), is of particular interest in terms of the structure and intensity of the mean flows. For example, the excitation of parametric instability of the interface of low-viscosity liquids undergoing high-frequency oscillations in a vertical slit gap leads to the generation of intense mean flows in relatively thin Stokes layers near the gap walls (Kozlov et al. 2024a, b). Moreover, the mean flows enhance mass transfer by several orders of magnitude (Dyakova et al. 2025). When the liquids oscillating in a slit channel have a high viscosity contrast, another type of interfacial instability can be excited: the oscillatory Saffman–Taylor instability (Kozlov et al. 2020; Kozlov and Vlasova 2022; Subbotin et al. 2023). This type of instability also leads to intense mixing of the liquids near the interface and to significant intensification of mass transfer across the interface.

The case of an interface between highly viscous liquids is a special case. For such an interface, the instability mechanisms listed above do not apply. Moreover, the oscillations themselves, in particular, high-frequency inertial oscillations of liquids with different densities, are impossible. In this regard, of interest is the situation in which the oscillations of the liquid and the interface are directly excited by a body oscillating at the interface. Ivanova et al. (1998) and Lyubimova et al. (2025) found that when a body with edges whose radius of curvature is less than the Stokes layer thickness oscillates, mean flows in the direction opposite to that of "steady streaming" are generated near the edges. It is clear that this case goes beyond the well-known and well-developed high-frequency asymptotic theory. The experiments of Ivanova et al. (1998) showed that when a body with an edge touching the surface of a viscous liquid oscillates, intense non-wave surface flows spread from the body along the interface. Surprisingly, their intensity did not decrease with increasing viscosity but, in certain situations, even increased. It should be noted that a sign reversal of the mean effects in the transition from high to low dimensionless frequencies is common to various vibration-induced effects: a change in the direction of the mean flows in an oscillating liquid (Vlasova et al. 2020) and a change from an averaged attractive force to a repulsive one for a body oscillating in a liquid (Schipitsyn and Kozlov 2018; Vlasova and Kozlov 2023).

It is the observation reported in Lyubimova et al. (2025) that forms the basis of the proposed study, the ultimate goal of which is to develop a method for intensifying mass transfer across the interface between high-viscosity liquids by generating mean flows with a body oscillating at the interface.

Experimental setup and methodic

The dynamics of two immiscible viscous liquids is experimentally studied in a flat vertical cell (Fig. 1). The cell is formed by two glass plates *1* measuring 200×110×10 mm and a plexiglass spacer *2* measuring 200×170×10 mm placed between them. The working cell is formed by a rectangular hole cut in the spacer, with a height $H = 80$ mm and a length $L = 100$ mm. The spacer thickness determines the cell thickness and is $A = 10$ mm. The setup is assembled using two pairs of clamping plates *3*, which are secured by bolts. To seal the working cell, an elastomeric thread *4* is used, laid along all sides of the cell. The cell is filled sequentially with two highly viscous immiscible liquids through filling holes *5* in the spacer. The liquid interface is set at a height of $H/2$. Castor oil ($\rho_1 = 0.95$ g/cm³, $\nu_1 = 8.5$ St) and glycerol ($\rho_2 = 1.26$ g/cm³, $\nu_2 = 8.0$ St) are used as the working fluids. A plexiglass body *6* in the form of a parallelepiped (thickness $a = 8.0$ mm, length $2l = 25.0$ mm) is located at the interface. Two types of plates are used: with right-angled edges and with a 4.5-mm-wide chamfer cut at 60°. The first plate has a height $h = 2.0$ mm; the second, $h = 7.0$ mm. The plate is mounted on a 1-mm-thick rod *7*, connected through a clamp *8* to a 300 W loudspeaker *9*. The speaker is mounted on a platform *10* and is controlled by a low-frequency signal generator paired with an amplifier. In the experiments, the oscillation frequency of the body is varied over the range $f = 20$–80 Hz, and the amplitude over $b = 0$–2 mm. At each frequency and amplitude step, video recording of the experiment is performed.

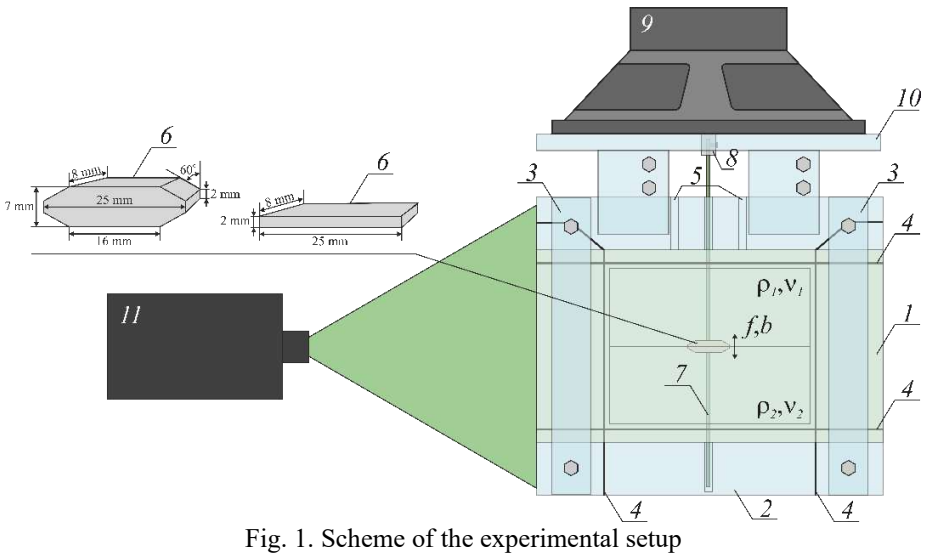
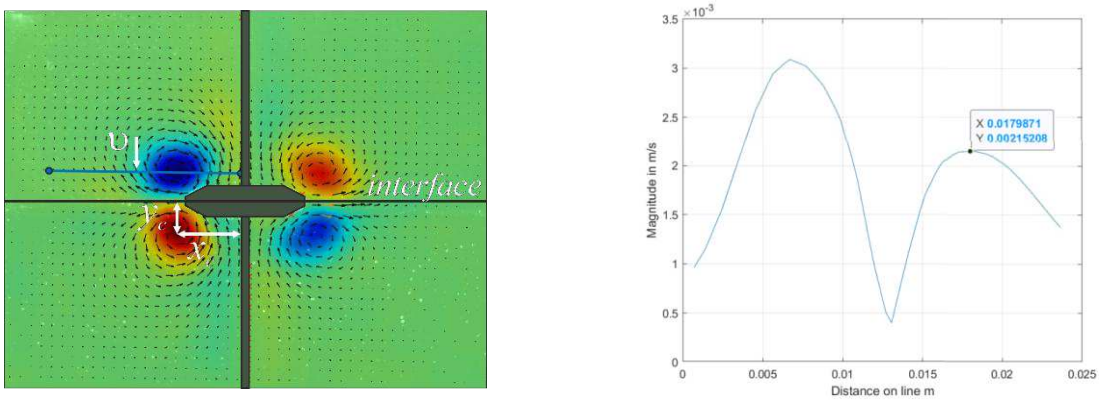


Fig. 1. Scheme of the experimental setup

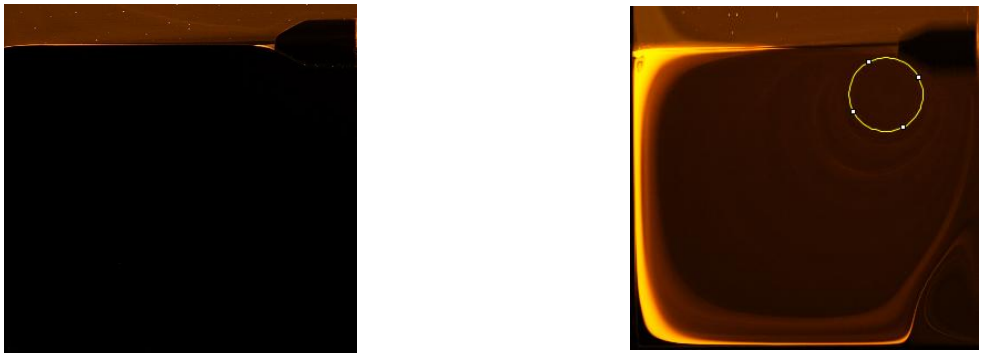
To study the flow structure, plastic light-reflecting particles are added to both liquids. The qualitative and quantitative study of the flow structure is carried out using the PIV technique (Thielicke and Stamhuis 2015) in a cross-section at the mid-thickness of the cavity, created by a 3-mm-thick green laser sheet *11*. The experiment is recorded with a VisCam NP-170UM high-speed camera, which operates at a frame rate equal to the frequency of the body oscillations. After processing the PIV data, the velocity and vorticity fields averaged over the oscillation period are obtained (Fig. 2, *a*). The velocity magnitude is measured along a line drawn parallel to the interface through the center of the vortex, in the direction from the center of the rod to the edge of the cell. To quantify the intensity of the vortex flow, the maximum liquid velocity υ at the outer edge of the vortex is taken from the measured velocity profile (Fig. 2, *b*). The experiments also track the horizontal x_c and vertical y_c coordinates of the vortex center. The x_c coordinate is measured from the rod, and the vertical coordinate from the interface. Such measurements are performed in both liquids.



a *b*

Fig. 2. Velocity field (color shows vorticity) at f = 40 Hz and b = 0.92 mm, with the measurement line indicated (*a*); magnitude of the averaged flow velocity along the line (*b*)

To study the mass transfer across the interface, a passive dye, rhodamine B, is added to castor oil; it dissolves completely in both liquids (down to the molecular level). When dissolved rhodamine B is illuminated with green laser light, its intense orange fluorescence is observed (Fig. 3). The linear dependence of the rhodamine B fluorescence intensity on concentration, determined previously in calibration experiments, makes it possible to obtain concentration data in the region of interest from the fluorescence brightness. A Fujifilm X-E4 color camera with an orange filter mounted in front of the lens is used to record the experiment. The filter blocks stray light from the laser and allows the rhodamine B fluorescence to be imaged. Image acquisition is performed at a rate of 1 frame per minute with a 1/40 s exposure, while the body oscillates at 40 Hz. Recording lasts 8 hours (480 frames). The initial concentration of rhodamine B in castor oil is C = 10.4 μmol/L. Immediately after filling the cell, fluorescence of rhodamine B is observed in the glycerol layer at the interface with the oil (the orange thin layer above the interface in Fig. 3, *a*). The photograph fragment shows the lower left quarter of the cell. The black color of the glycerol in the photograph indicates the complete absence of rhodamine B in it. Since, in the presence of body oscillations, the volumetric transfer of rhodamine B into the glycerol occurs unevenly (Fig. 3, *b*), the brightness averaged over the area inside a 10-mm-diameter circle (shown in Fig. 3, *b*) is measured to quantify the amount of transferred substance. The size and position of the circle are determined by the region where the most intense time-averaged fluid motion is concentrated.



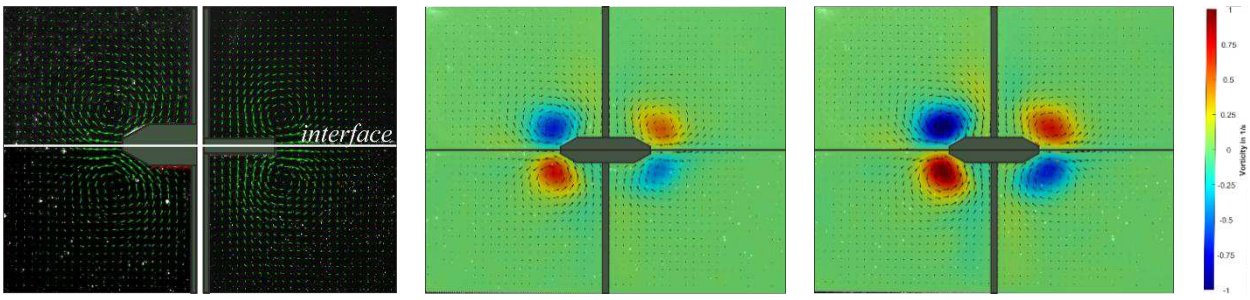
a *b*

Fig. 3. Photograph of the rhodamine B distribution in the lower-left quarter of the cell: t = 0 (*a*) and t = 200 min (*b*); f = 40 Hz, b = 0.82 mm

Experimental results

Mean flow

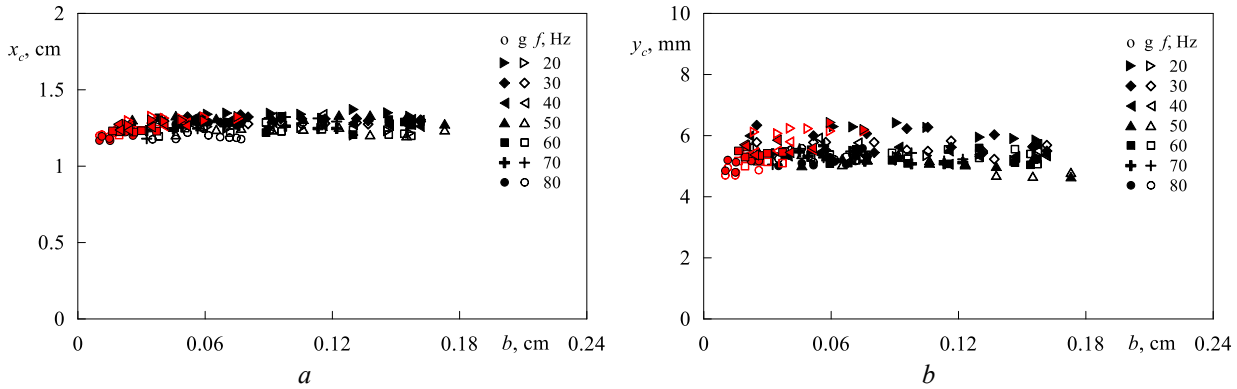
At the beginning of the experiment, the liquids are in a stable configuration: light oil on top, heavy glycerol at the bottom. The interface is horizontal and lies along the axis of symmetry of the body. The body vibrations generate two mean jets that separate from the edges of the vibrating body and spread in the plane of the layer away from the body along the interface in opposite directions. A pair of large-scale vortices of opposite spin is generated in each liquid (Fig. 4, *a*). Note that the shape of the body does not affect the structure of the generated mean flow; the flow structure and intensity, as will be shown below, are practically the same for both bodies (see Fig. 4, *a*). As the amplitude of the body oscillations increases, the intensity of the generated flow increases (Fig. 4, *b*–*c*). The color in the figures shows the flow vorticity; the scale is given on the right. Fragments (*a*), (*b*), and (*c*) correspond to body-vibration amplitudes $b = 0.54$, 0.73, and 0.92 mm, respectively, and to a frequency $f = 40$ Hz. The intensity of the mean flow decays rapidly with distance from the oscillating body, owing to the high viscosity of the liquids.



a *b* *c*

Fig. 4. Velocity vector field (*a*) and vorticity fields (*b*, *c*) at $f = 40$ Hz: $b = 0.54$ (*a*), 0.73 (*b*), 0.92 mm (*c*)

The structure of the mean flow remains almost unchanged over the entire studied range of body oscillation frequencies and amplitudes. Figure 5 shows plots of the horizontal x_c (*a*) and vertical y_c (*b*) coordinates of the vortex center versus the body oscillation amplitude at various oscillation frequencies. Measurements were performed in the oil and glycerol in the left half of the cell. Here and below, empty symbols refer to glycerol and filled symbols to oil. The red symbols represent data obtained with the right-angled plate, and the black symbols those for the beveled plate. It can be seen that, regardless of the frequency and amplitude of the body oscillations, the position of the vortex center in both the vertical and horizontal directions remains within the same range, without a pronounced systematic shift. The shape of the body also has no effect on the location, size, and shape of the vortices. Note that the x_c and y_c coordinates differ slightly between the liquids. This is due to the slight difference in the physical properties of the liquids used, primarily their kinematic viscosity. However, for a given liquid, the coordinates x_c and y_c remain almost constant when the experimental parameters change. Note that $x_c \approx l$, which indicates the key role of the body edge in positioning the generated vortex. The vertical position of the vortex center, measured in Stokes boundary-layer thicknesses, is 2–3δ. As the amplitude or frequency of the oscillations increases, the fluid velocity increases and, accordingly, the intensity of the vortical flows; however, the geometric structure of the flow and the location of the vortex regions relative to the oscillation axis remain virtually unchanged.



a *b*

Fig. 5. Horizontal x_c and vertical y_c coordinates of the vortex center versus the body oscillation amplitude at various oscillation frequencies

The maximum velocity υ at the outer edge of the vortex is chosen as the characteristic velocity of the generated mean flow (see the description of the experimental procedure). Experiments have shown that, at a fixed body oscillation frequency and regardless of its shape, the characteristic velocity of the mean fluid flow increases in

proportion to the square of the body oscillation amplitude (Fig. 6). The measurement error does not exceed the size of the symbol and is not shown in the graph. Figure 6, *a* presents the data obtained with the right-angled plate, and Fig. 6, *b* those obtained with the beveled plate. The similar velocities for glycerol and oil are due to their similar viscosities. As the oscillation frequency decreases, the intensity of the mean flow decreases. It should be noted that, as shown above, when the oscillation amplitude changes, the position of the vortices does not change. The main change is an increase in the intensity of the mean motion. In addition, the results obtained demonstrate that the oscillation amplitude is one of the governing parameters affecting the intensity of mean flows in highly viscous liquids.

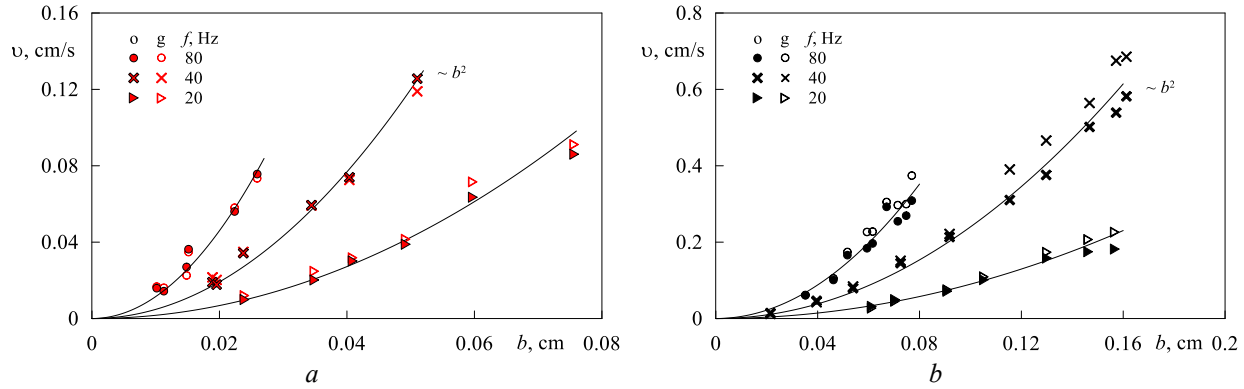
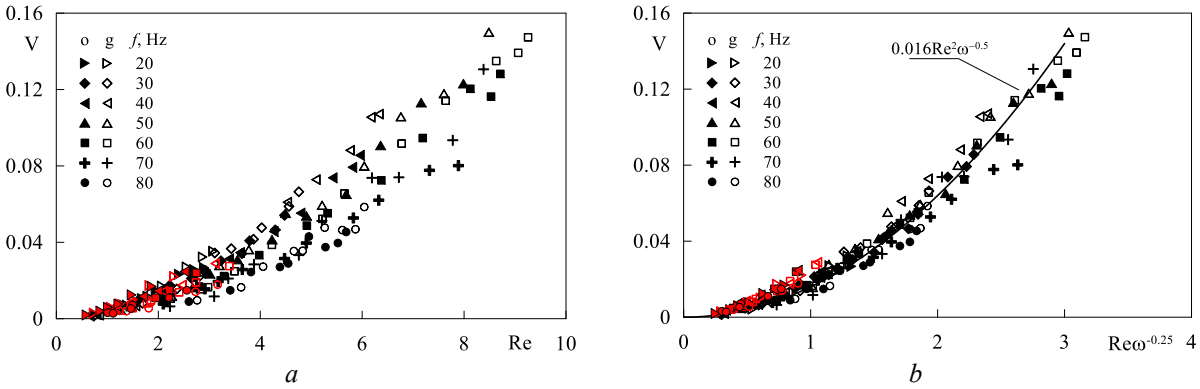


Fig. 6. Maximum fluid flow velocity versus the oscillation amplitude at various oscillation frequencies: (*a*) right-angled plate; (*b*) beveled plate

The mechanism of mean flow generation by a body oscillating in a viscous liquid differs from the mechanisms known and described in the Introduction for high frequencies. In our case, the Stokes layer thickness is about 1.5 – 3.5 mm, and since the liquids have similar viscosities, the boundary layers differ only slightly. The Stokes layers in both liquids are an order of magnitude smaller than the body dimensions; however, the flow structure is qualitatively different from that known for high frequencies [6]. This is due to the fact that the relatively sharp edges of the oscillating plate and, presumably, the separation nature of the oscillatory motion of the liquids play a decisive role. The radius of curvature of the sharp edges is an order of magnitude smaller than the Stokes layer thickness. It can be assumed that the vorticity generated in the boundary layers is injected into the surrounding liquid at a certain phase of the period, and this injection acts as the generator of the mean vortex flow. This may explain the quadratic dependence of the flow intensity on the oscillation amplitude at a given frequency (see Fig. 6). Note that the mean flows generated by direct injection of vorticity from the boundary layer at a certain phase of the period should be significantly more intense than the mean secondary flows known as "steady streaming."

A summary of the experimental data obtained in this study is presented in the plane of dimensionless parameters (Fig. 7, *a*). The velocity υ is made dimensionless using half the plate length *l* and the kinematic viscosity ν, as $V = \upsilon l/\nu$. The Reynolds number $\mathrm{Re} = b\Omega l/\nu$, defined in terms of the velocity of the body's oscillatory motion, is chosen as the governing parameter. The results obtained for both castor oil and glycerol collapse onto a single dependence at f = const. This indicates a common mechanism of mean flow formation in the studied range of experimental parameters. However, the experimental data are stratified owing to the variation in oscillation frequency. A satisfactory data collapse is obtained in the plane of the dimensionless parameters $V(\mathrm{Re}\omega^{-0.25})$ (Fig. 7, *b*). It can be seen that the dimensionless velocity characterizing the intensity of the generated mean flow increases in proportion to the square of the dimensionless complex $\mathrm{Re}\omega^{-0.25}$. The square of this dimensionless parameter can be written as follows: $\mathrm{Re}^2\,\omega^{-0.5} = \frac{b^2\Omega^2 l^2}{\nu^2}\frac{\sqrt{\nu}}{l\sqrt{\Omega}} = \frac{b^2 l\delta}{\delta^4} = \left(\frac{b}{\delta}\right)^2\frac{l}{\delta}$. This allows one to conclude that, in the studied region of low dimensionless frequencies (the radius of curvature of the oscillating body edge is much smaller than the Stokes layer), the relative amplitude of the body oscillations (b/δ) and its relative longitudinal dimension l/δ play a key role in the generation of the mean flow.



a *b*

Fig. 7. Dimensionless characteristic fluid flow velocity versus the dimensionless parameters

Masstransfer

The procedure for studying the transfer of the dye (rhodamine B) across the interface was as follows. The experiments were carried out with a solution of rhodamine B in castor oil at a concentration of C = 10.4 μmol/L and with pure glycerol. First, glycerol was poured into the cell (up to the mid-height of the body), and then the rhodamine solution in castor oil was added. Both liquids were illuminated through the side wall of the cell by a vertical green laser sheet. The rhodamine concentration in both media could be inferred from the intensity of its fluorescence, which lay in the orange range.

In the first stage (in the absence of body vibrations), photographic recording was performed once every few hours. Figure 8 shows fragments of photographs taken in the absence of vibrations immediately after pouring (*a*) and three days later (*b*). The photographs show a relatively faintly fluorescing castor oil (above the interface) and a brightly fluorescing interface, more precisely, a thin glycerol layer into which rhodamine has diffused. Outside the bright layer, the black color of the glycerol indicates the complete absence of rhodamine B in it. The brighter fluorescence of rhodamine B at the interface is explained by the fact that the fluorescence efficiency of rhodamine B in glycerol significantly exceeds that in castor oil. It can be seen that over the specified time (three days), the distribution of rhodamine B in the glycerol changed only slightly: the bright band expanded deeper into the liquid. The small penetration depth of rhodamine B over a long period is explained by its transfer occurring via diffusion. Data found in the open literature on the diffusion coefficient of rhodamine B in glycerol give a value of D ~ 10^{-9} cm^2/s.



a *b*

Fig. 8. Photographs of the rhodamine B distribution near the interface: t = 0 (*a*) and t = 3 days (b)

Once the body vibrations are switched on and the mean flows are excited, these flows entrain rhodamine B from the boundary layer near the interface and transport it into the bulk of the glycerol. The experiments were performed at an oscillation frequency f = 40 Hz. Regardless of the plate oscillation amplitude, the transfer of rhodamine B in the glycerol occurs unevenly (Fig. 9). Figure 9 shows a series of photographs of the lower-left quarter of the cell 200 and 400 min after the body vibrations are switched on, for different plate oscillation amplitudes. The photographs show regions of varying fluorescence intensity, which indicates different rhodamine B concentrations within the cell.

Some features of mass transfer in the system under consideration should be noted. The rhodamine concentration in the glycerol (inferred from its fluorescence) near the interface increases with distance from the vibrating body, which generates the radial tangential motion of the interface (Fig. 9). No fluorescence is observed near the body, in the region of maximum radial velocity of the interface. This is because rhodamine needs time to diffuse across the interface newly formed near the body. With distance from the body, the velocity decreases, and the fluorescence brightness (the mass of rhodamine that has passed into the glycerol) increases. The highest fluorescence intensity of rhodamine B is observed in regions with low fluid velocity: in the layers near the interface at the side walls of the cell, and also at the periphery of the vortex motion, where glycerol saturated with rhodamine is transported. The rate of molecular diffusion is insufficient for rhodamine B to penetrate directly through the boundary layers into the bulk of the liquid; therefore, it spreads by transport. When the body oscillates, the generated mean flow carries the glycerol layer near the interface, into which rhodamine B has diffused, toward the side wall of the cell. The higher the body oscillation amplitude, the more intense the generated flow and the further rhodamine B is carried along the interface. As the fluid decelerates along the interface, its fluorescence increases, indicating an increase in rhodamine B concentration. As a result, a stagnation zone forms at some distance from the body, from which rhodamine B is slowly removed and spreads along the periphery of the generated vortex.

The rate of rhodamine B transport in the cell depends on the intensity of the generated mean flow. As described in the previous section, the higher the body oscillation amplitude, the more intense the mean fluid motion and, hence, the faster the rhodamine B transfer. Within t = 200 min, at an amplitude b = 0.28 mm, rhodamine B penetrated only 1.5 cm into the liquid, whereas at b = 0.46 mm it had already reached the bottom of the cell. However, until rhodamine B reaches the vortex core (the region of maximum fluid flow intensity), there is practically no saturation of the entire liquid volume with the dye (as observed at b = 0.28 and 0.46 mm). At an amplitude b = 0.82 mm, within 200 min of the experiment, rhodamine B reached the vortex core and spread, at a certain concentration, throughout the entire cell volume, as evidenced by the faint fluorescence of the entire cell. With further elapsed time, the concentration field becomes almost homogeneous (t = 400 min).

It is also worth noting the important role of the cell size and the scale of the generated flow. The scale of the vortex motion can be inferred from the rhodamine B distribution in the cell (t = 400 min). At sufficiently large amplitudes (b = 0.46 and 0.82 mm), the vortex motion of the fluid occupies the entire cell volume. Moreover, the larger b, the thinner the boundary layers on the cell walls: the photographs clearly show the difference in thickness of the bright rhodamine B bands spreading along the cell walls. At low body oscillation amplitudes (b = 0.28 mm), the vortex motion does not reach the side walls of the cell. In this case, the entrainment of rhodamine B deep into the glycerol occurs at some distance from the cell wall. The vortex size turns out to be smaller than the cell dimensions; as a result, stagnation zones (black regions) are observed near the side and bottom walls of the cell, indicating the absence of rhodamine B. Despite this, the mechanism of dye propagation remains the same: the dye is transported along the periphery of the vortex, and upon reaching the vortex core, it spreads throughout the volume almost uniformly. With time, the regions near the cell walls are gradually filled with rhodamine B.

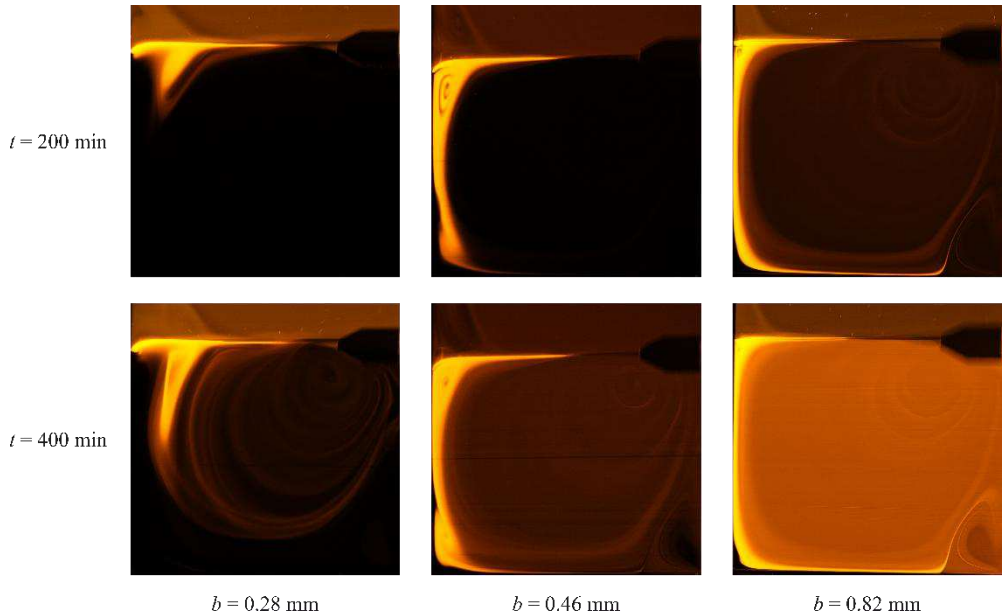


Fig. 9. Photograph of the rhodamine B distribution in the lower-left part of the cell; the time elapsed since the start of the experiment is indicated on the left and the amplitude at the bottom

For the three body oscillation amplitudes presented above, the amount of rhodamine B transferred over time in the region of the most intense vortex motion was quantified (see the experimental procedure). Figure 10 shows the time variation of the area-averaged rhodamine B concentration for different body oscillation amplitudes. It can be seen that the curves show a similar trend. At the beginning of the experiment, the rhodamine B concentration in the region of interest remained virtually unchanged. After a certain time, the dye concentration begins to grow rapidly. As mentioned above, active saturation of the surrounding liquid with the dye occurs only when rhodamine B trapped at the interface reaches the vortex core. Moreover, the higher the body oscillation amplitude, the less time is required to deliver rhodamine B to the region of interest. The kink in the curve characterizes the time of one fluid revolution at the vortex periphery. The upper horizontal axis of the graph indicates the experimental time normalized to the diffusion time τ, calculated as $\tau = H^2/4D$. It can be seen that the time required for the dye to spread throughout the cell volume is many orders of magnitude shorter than the diffusion time. This indicates the high efficiency of the proposed vibration-based method for mass transfer intensification.

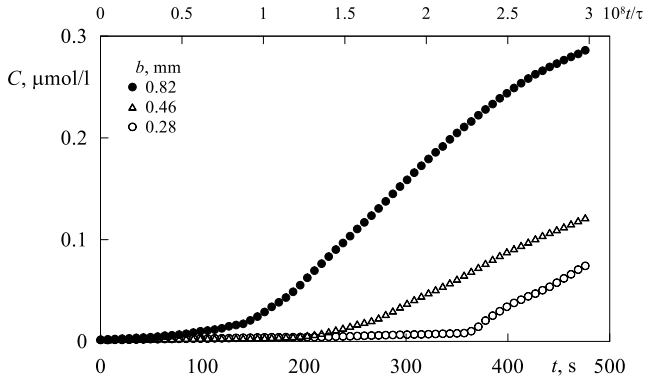


Fig. 10. Rhodamine B concentration in the glycerol vortex core versus time

Conclusion

An experimental study of the mean flows generated by normal oscillations of a body located at the interface between high-viscosity liquids has been carried out. The experiments were performed in a flat rectangular cell. It has been found that body oscillations lead to the generation of intense mean flows in both liquids: localized vortices form near the sharp edges of the oscillating body and, in the plane of the layer, are arranged symmetrically with respect to the interface and the vibrating body. It is shown that the intensity of the mean flow increases in proportion to the square of the body oscillation amplitude. The observed mean flows are qualitatively different from those known as "steady streaming," excited by oscillating bodies in low-viscosity liquids. It is found that the intensity of the observed mean vortices increases with the Stokes layer thickness according to $V \sim (b/\delta)^2 * l/\delta$, where V is the dimensionless flow velocity, b is the body oscillation amplitude, and l is the body size. It is shown that the shape of the body does not play a decisive role; what matters is the presence of sharp edges on the body. The discovered phenomena and regularities are new; they are of great scientific interest and require further theoretical and experimental study.

It was found that intense mean vortices localized near the edges of the vibrating body impart motion to the liquid throughout the entire cell. This qualitatively changes and intensifies the transfer of a passive dye from one liquid to the other. It is shown that the rate of mass transfer across the interface in the presence of a vibrating body increases by several orders of magnitude compared with diffusive mass transfer in the absence of vibrations. The discovered effects are new; they are of scientific interest from a fundamental standpoint and have significant application potential as a method for intensifying mass transfer across the interface between viscous liquids by localized vibrational forcing.

Funding: The study was financially supported by the Russian Science Foundation (Grant No. 23-11-00242-P).

Data Availability: Data available on request from the corresponding authors.

Declarations

Conflicts of interest: The author declares no conflicts of interest to report regarding the present study.

Authors' contributions: V.K. set up the experiment; O.V., A.V., V.K. ran experiments and took measurements; O.V. performed image and data processing; V.K. acquired funding; all authors performed analysis of experimental results, wrote the main manuscript text; all authors reviewed the manuscript.

Ethics approval: Not applicable.

Consent to participate: Not applicable.

References

Batchelor, G.K.: An introduction to fluid dynamics. Cambridge University Press, Cambridge University Press (1967)

Denisova, M. O., Kostarev, K. G., Torohova, S. V.: The influence of chemical potential differences on the development of mass transfer in liquid systems with an interphase boundary. Microgravity Sci. Technol. 38(5), 75 (2026) https://doi.org/10.1007/s12217-026-10294-9

Denisova, M., Kostarev, K. Peculiarities of mass transfer between the droplet with a chemical reaction on its surface and the surrounding medium. Microgravity Sci. Technol. 34(5), 84 (2022) https://doi.org/10.1007/s12217-022-09992-x

Dyakova, V.V., Vlasova, O.A., Kozlov, V.G.: Experimental study of mass transfer through an oscillating interface of immiscible liquids. Konvektivnye techeniya (2025) 12, 19-32 (in Russian)

Ivanova, A.A., Kozlov, V.G., Lyubimov, D.V., Lyubimova, T.P., Meragy, S., Roux, B.: Structure of averaged flow driven by a vibrating body with a large-curvature edge. Fluid Dyn. 33(5), 659–665 (1998) https://doi.org/10.1007/bf02698614

Kozlov, N.: Vibrational heat transfer intensification in an annulus with a deformable boundary. Shock Vib. 2019(1), 9108795 (2019) https://doi.org/10.1155/2019/9108795

Kozlov, V., Karpunin, I., Kozlov, N.: Finger instability of oscillating liquid–liquid interface in radial Hele-Shaw cell. Phys. Fluids 32(10), 102102 (2020) https://doi.org/10.1063/5.0018541

Kozlov, V., Vlasova, O., Dyakova, V.: Oscillatory excitation of Faraday waves on the interface of immiscible fluids in a slotted channel. Phys. Fluids 36(10), 102117 (2024a) https://doi.org/10.1063/5.0230721

Kozlov, V., Vlasova, O.: Oscillatory dynamics of immiscible liquids with high viscosity contrast in a rectangular Hele-Shaw channel. Phys. Fluids 34(3), 032121 (2022) https://doi.org/10.1063/5.0084363

Kozlov, V.G., Kozlov, N.V., Schipitsyn, V.D.: Steady flows in an oscillating deformable container. Effect of the dimensionless frequency. Phys. Rev. Fluids 2, 094501 (2017) https://doi.org/10.1103/physrevfluids.2.094501

Kozlov, V.G., Vlasova, O.A., Dyakova, V.V.: Stability of the interface of liquids oscillating in a vertical flat channel. Interfacial Phenom. Heat Transf. 12(1) (2024b) https://doi.org/10.1615/interfacphenomheattransfer.2023049906

Landau, L.D., Lifshitz, E.M.: Fluid Mechanics. Pergamon Press, Oxford (1959)

Lyubimov, D.V., Lyubimova, T.P., Cherepanov, A.A.: Dynamics of Interfaces in Vibration Fields. FizMatLit, Moscow (2003) (in Russian)

Lyubimova, T., Lyubimov, D., Ivanova, A., Kozlov, V., Meragy, S., Roux, B.: Mean flows induced by oscillations of a solid body immersed in an isothermal liquid. Microgravity Sci. Technol. 37(4), 45 (2025) https://doi.org/10.1007/s12217-025-10197-1

Nyborg, V.: In: Mason, W.P. (ed.) Physical Acoustics, vol. 11, part B. Academic Press, New York (1965)

Rayleigh, L.: On the circulation of air observed in Kundt's tubes, and on some allied acoustical problems. Philos. Trans. R. Soc. Lond. 175, 1–21 (1884) https://doi.org/10.1098/rstl.1884.0002

Riley, N.: On a sphere oscillating in a viscous fluid. Q. J. Mech. Appl. Math. 19(4), 461-472 (1966) https://doi.org/10.1093/qjmam/19.4.461

Riley, N.: Steady streaming. Annu. Rev. Fluid Mech. 33(1), 43–65 (2001) https://doi.org/10.1146/annurev.fluid.33.1.43

Sabirov, R.R., Kozlov, V.G., Subbotin, S.V.: Steady flows in an oscillating spheroidal cavity with elastic wall. Fluid Dyn. 53, 189–199 (2018) https://doi.org/10.1134/s0015462818020118

Schipitsyn, V., Kozlov, V.: Oscillatory and steady dynamics of a cylindrical body near the border of vibrating cavity filled with liquid. Microgravity Sci. Technol. 30(1–2), 103–112 (2018) https://doi.org/10.1007/s12217-017-9583-4

Schlichting, H.: Grenzschicht-Theorie. Braun, Karlsruhe (1951)

Subbotin, S., Karpunin, I., Kurysheva, D., Kozlov, V.: Effect of the density ratio on the oscillatory Saffman–Taylor instability in vertical conical Hele-Shaw cell. Phys. Fluids 35(9), 093102 (2023) https://doi.org/10.1063/5.0162264

Subbotin, S.V., Kozlov, V.G., Sabirov, R.R.: Steady flows in deformed elastic sphere subject to rotational oscillations. Phys. Fluids 30(9), 093606 (2018) https://doi.org/10.1063/1.5048789

Taneda, S.: Visual observation of the flow around a half-submerged oscillating sphere. J. Fluid Mech. 227, 193–209 (1991) https://doi.org/10.1017/s0022112091000083

Taneda, S.: Visual observations of the flow around a half-submerged oscillating circular cylinder. Fluid Dyn. Res. 13(3–4), 119–151 (1994) https://doi.org/10.1016/0169-5983(94)90046-9

Thielicke, W., Stamhuis, E.J.: PIVlab – time-resolved digital particle image velocimetry tool for MATLAB (version: 3.12). (2014)

Van Dyke, M.: An Album of Fluid Motion. The Parabolic Press, Stanford (1982) https://doi.org/10.1115/1.3167071

Vlasova, O., Kozlov, V., Karpunin, I., Latyshev, D.: Steady flows of a fluid oscillating in an axisymmetric channel of variable cross-section, versus the dimensionless frequency. Microgravity Sci. Technol. 32(3), 363–368 (2020) https://doi.org/10.1007/s12217-019-09775-x

Vlasova, O., Kozlov, V.: Experimental study of the solid motion in the vicinity of the wall in an oscillating cavity. Microgravity Sci. Technol. 35(4), 38 (2023) https://doi.org/10.1007/s12217-023-10062-z

Volodin, I., Alabuzhev, A.: Mass transfer simulation in an inclined two-layer porous channel by the lattice Boltzmann method. Microgravity Sci. Technol. 37(5), 47 (2025) https://doi.org/10.1007/s12217-025-10200-9